Research Square

Preprints are preliminary reports that have not undergone peer review.
They should not be considered conclusive, used to inform clinical practice,
or referenced by the media as validated information.

Assessment of the impact of cellulose, adhesive labels and metals on the chemical recyclability of high-impact polystyrene from yogurt cups

Saddys Rodríguez Llamazares

s.rodriguez@cipachile.cl

Centro de Investigación de Polímeros Avanzados

Mario I. Sanhueza

Centro de Investigación de Polímeros Avanzados

Constanza Sabando

Centro de Investigación de Polímeros Avanzados

Diego Ricciardi

Centro de Investigación de Polímeros Avanzados

Serguei Alejandro-Martín

University of Bío-Bío

Rebeca Bouza

University of A Coruña

Sonia Dopico

University of A Coruña

Natalia Pettinelli

Centro de Investigación de Polímeros Avanzados

Edgar Pastene

University of Bío-Bío

Eliezer Velásquez

University of Santiago Chile

Research Article

Keywords: High impact polystyrene, non-catalytic pyrolysis, cellulose and adhesive, chemical recyclability

Posted Date: April 9th, 2026

DOI: https://doi.org/10.21203/rs.3.rs-9234165/v1

License: This work is licensed under a Creative Commons Attribution 4.0 International License.
Read Full License

Additional Declarations: No competing interests reported.

Version of Record: A version of this preprint was published at Journal of Polymers and the Environment on September 27th, 2026. See the published version at https://doi.org/10.1007/s10924-026-03970-9.

Abstract

Trace amounts of auxiliary food packaging components, such as paper adhesives and inks, limit the ability to selectively produce value-added products through chemical recycling. This study evaluates the effect of paper labels, adhesive residues and metal pollutants from labels and additives used in the manufacture of yogurt cups on the degradation products resulting from the chemical recycling of post-consumer HIPS food packaging via non-catalytic pyrolysis. Five Chilean dairy manufacturers were selected as sources for post-consumer yogurt cups. In addition, cups containing labels, cups containing adhesive residues and clean cups were considered. FTIR-ATR combined with Principal Component Analysis (PCA) confirmed that post-consumer cups have a similar chemical structure and minimal food contamination. The polystyrene fractions in post-consumer cup waste exhibited a similar molecular weight distribution (Mn = 87–105 kDa and Mw = 230–280 kDa). According to TGA analysis, the adhesive residue and labels decrease the stability of post-consumer HIPS samples and contribute to the formation of stable carbon residues above 690°C. Al, Fe, Ti, Zn and Cr were quantified by ICP-MS. Zn (50–116 μg g^{-1}) was potentially related to the transformation of HIPS material into food packaging. Non-catalytic pyrolysis produced predominantly aromatic hydrocarbons (70–98% relative area), with styrene being the main compound. Cups containing labels yielded a broader range of products and minor oxygenated compounds, whereas cleaner cups showed higher styrene selectivity than virgin HIPS used as a reference. Overall, Chilean yogurt cup waste is a promising feedstock for producing styrene via non-catalytic cracking, although super clean methods are recommended beforehand.

Introduction

Polystyrene accounts for around 7% of the global plastic market. In 2023, 21 million tons were produced and it is estimated that 25% of this is destined for the packaging industry [1, 2]. This plastic is commercially available in three forms: expanded polystyrene, general-purpose polystyrene, and high-impact polystyrene (HIPS). The last is one of the most cost-effective thermoplastic polymers for food packaging due to its good balance of impact resistance, rigidity and elasticity, low moisture uptake, low density, ease of processing, and printability [3]. However, the short lifespan of most polystyrene packaging results in widespread disposal, raising environmental concern. The disposal of polystyrene packaging in aquatic and soil environments can also lead to contamination by toxic substances, either intentionally added during manufacturing or unintentionally adsorbed during the packaging's lifecycle. Of particular concern is the ingestion of polluting polystyrene by marine organisms, as these toxic additives can accumulate in the aquatic food chain [1].

HIPS resin consists of a continuous polystyrene (PS)-rich matrix (glassy phase) and micron-sized domains of dispersed polybutadiene (PB)-rich phase containing PS occlusions (rubber phase). The rubber phase and PS occlusions are compatibilized with the PS-rich phase by a graft copolymer, PB-*g*-PS, formed during HIPS synthesis [4, 5]. The rubber phase, in the range of 3–8 mol %, [6] contributes to enhancing the impact strength and toughness of the glassy polystyrene phase. However, during mechanical recycling, the rubber phase's parameters, such as gel content, grafting degree, and swelling

index, decline significantly, resulting in recycled HIPS with inferior rheological and mechanical properties compared with virgin HIPS [7]. In addition, during the first mechanical recycling, cross-linking reactions involving the rubber´s double bonds increase the rigidity of the rubber domains, resulting in a reduction in impact performance [8].

Thermal and mechanical degradation during the extrusion process limit the applicability of HIPS for mechanical recycling [9]. In addition, post-consumer HIPS food packaging does not qualify for direct, and high-quality mechanical recycling due to the inherent heterogeneity of HIPS, as well as the presence of auxiliary packaging components, such as adhesive tapes and shipping labels, which enhance sealing and traceability [1, 5, 6]. Although the mass proportion of some of the auxiliary components of the packaging, such as adhesives and inks, is small, the recyclability of the primary packaging is greatly hindered due to their complex structure and strong adhesiveness, as well as the risk of heavy metal contamination [7].

Chemical recycling is an alternative for dealing with heterogeneous plastic waste streams, such as post-consumer HIPS from food packaging. One method of chemical recycling is pyrolysis, which involves heating in an oxygen-starved environment. The major product of polystyrene pyrolysis is styrene [1, 10]. The C-C bonds in the benzene ring of the PS backbone have a low activation energy (20–77 kcal mol^{-1}), meaning that the aliphatic carbon bonds between adjacent aromatic rings are selectively broken. Other compounds obtained from the pyrolysis of PS include benzene, toluene, ethylbenzene and xylenes (BTEX) [11]. Most reports on HIPS focus on the effects of halogenated flame retardants on pyrolyzates. Additives present in HIPS are derived from waste electric and electronic equipment. Catalytic and non-catalytic pyrolysis of HIPS containing halogenated flame retardants produces hazardous environmental pollutants, including polycyclic aromatic hydrocarbons, hydrogen bromide, and polybrominated diphenyl ethers or esters [12]. Some recent works focus on the co-pyrolysis of plastic and organic waste mixtures from contaminated environments, as well as on the use of pyrolysis coupled with gas chromatography-mass spectrometry (Py-GC/MS) to identify and quantify micro- and nanoplastics in these environments [13]. It has also been used to determine the degradation ranges of plastics and their degradation patterns [14].

One topic that has not been widely explored is the chemical recycling of post-consumer HIPS containers with paper labels. In Chile, for example, post-consumer yogurt cups contain around 20% paper by total mass. The paper label is difficult to remove, even after thorough washing; traces of labels and adhesives remain. It is known that the pyrolysis of clean paper/PS mixtures generates more syngas and energy than converting the components separately (i.e., paper and polystyrene) [15]. However, to our knowledge, there are no reports on the effect of paper labels and adhesives on the pyrolytic degradation of HIPS packaging compounds. Another issue to address is the impact of the metals from pigments, stabilizers and antioxidants used in the manufacture of these cups, as well as those from pigments in paper labels, on the distribution of degradation products during the non-catalytic pyrolysis of post-consumer HIPS cups. It should be noted that metal oxide-based catalysts influence the distribution of products obtained during PS pyrolysis [16, 17].

This study aims to evaluate the effect of paper labels, adhesive residues, and metal pollutants from labels and additives used in the manufacture of yogurt cups on the degradation products resulting from the chemical recycling of post-consumer HIPS food packaging via non-catalytic pyrolysis. First, post-consumer packaging will be classified using chemometric methods applied to Fourier transform infrared spectroscopy. This study will also involve a physical-chemical characterization of post-consumer packaging from different brands sold in Chile, including an analysis of metal content by inductively coupled plasma mass spectrometry (ICP-MS).

Material and methods

Materials

5 kg of post-consumer high-impact PS (HIPS) packaging from yogurt cups was provided by the company Triciclos, Chile. The cups were collected in April-May 2024 in Concepción city, Chile. Additionally, approximately 2 kg of yogurt cups were collected by workers at our research center. Virgin HIPS pellets, HI425E grade from Kumho Petrochemical Company, commercialized in Chile, were used as reference material.

Sample pre-treatment: Cleaning, hand classification and grounding

Five Chilean dairy manufacturers were first selected as the source of the post-consumer material collected for this study. Their yoghurt cups were then sorted by brand. The brands were Danone (D), Loncoleche (LL), Colun (C), Soprole (S) and Nestlé (N). The cups were then washed with tap water to remove any visible dirt. The cups were then dried at room temperature and weighed.

The cups were sorted by brand and immersed in distilled water for 24 hours as a second wash to eliminate any soluble food or non-food residues from the yogurt cups. The yogurt cup wastes were then subdivided into three groups (see Fig. 1). Group I in which no additional treatment was performed, and the cups were considered post-consumer with labels; Group II those for which the label was mechanically removed from the cups, which were then washed with tap water, dried and weighed. This group was considered post-consumer cups with adhesive residues, and Group III consisted only of the borders and bases cut off to obtain post-consumer HIPS free of adhesives and labels. Representative photographs of post-consumer yogurt cups, sample codes for groups, and the percentage of paper labels for each brand of yogurt cup are shown in Fig. 1.

Before homogenization, the percentage of label on the cups of each yogurt brand was determined by gravimetry, considering the mass of the whole yogurt cup with label (Group I) and after removing it (Group II). The samples, separated by brand and group, were cut by hand and then cryogenically ground using an IKA A11 Basic blade mill. The samples were sieved, and the fraction smaller than 425 μm was used for further analysis.

Sample characterization

The samples were first characterized by attenuated total reflectance-Fourier infrared spectroscopy (ATR-FTIR) to verify the plastic type and detect traces of contaminants in post-consumer packaging. Following the chemometric procedure detailed in Section 2.3.2., three new samples were considered by mixing post-consumer packaging from Groups II and III.

The samples were then characterized using gel permeation chromatography (GPC), a melt flow indexer, differential scanning calorimetry (DSC), thermogravimetric analysis (TGA), and ICP-MS (see Online Resource 1).

ATR-FTIR spectroscopy analysis

The FTIR analysis was carried out using attenuated total reflectance (ATR) with a PerkinElmer Spectrum Two spectrophotometer equipped with a diamond crystal. Spectra were collected in the 4000–400 cm^{-1} range with a resolution of 0.5 cm^{-1} and 32 scans per spectrum. All measurements were conducted at room temperature (with atmospheric correction), and a constant ATR head pressure of 91 force index was applied. The region chosen for FTIR spectra showed no visible folds or imperfections.

Fifteen random samples of the post-consumer yogurt cups from 5 brand types and HIPS virgin were analyzed in triplicate. The ATR- FTIR spectra were taken from different post-consumer cups and from different areas of the cups (Online Resource 1).

FTIR spectra preprocessing

The FTIR spectral dataset was truncated to 3200 - 400 cm^{-1}, and several pre-processing steps were carried out using custom-built in-house scripts in MATLAB R2023a (The MathWorks, Inc., USA). Firstly, the baseline was corrected using anchor points. Then, a Savitzky-Golay smoothing filter with degree 2 and window size 25 was applied, followed by normalization to the band at 1601 cm^{-1}, associated to aromatic C=C vibration in polystyrene [18]. After that, Standard Normal Variate (SNV) and mean centering were performed to reduce baseline variation in spectral measurements. The first derivative enhanced subtle spectral differences, and mean centering adjusted the dataset to have a zero mean. Followed, the 675–680 cm^{-1} and 1682–1687 cm^{-1} regions with spikes and random noise in the raw spectra were corrected via spline function according to reported by [19].

Multivariate statistical analysis for FTIR

Principal Component Analysis (PCA) was applied to the preprocessed FTIR dataset to explore variance patterns associated with: (1) the type of HIPS used to manufacture yogurt cups of different commercial brands, using the FTIR spectra of the clean outside surfaces of all yogurt cups; (2) food contamination using the FTIR spectra of the inside of all yogurt cups; and (3) label and adhesive residues using the FTIR spectra of the dirty outside surfaces of all yogurt cups. The PCA analysis included 70 FTIR spectra.

PCA was performed in MATLAB R2023a using in-house scripts based on Singular Value Decomposition (SVD). Outlier samples were identified using a combination of Mahalanobis Distance and the Sample

Residual test. The outlier samples were removed from the PCA. The three principal components were determined based on the cumulative explained variance for the classification by HIPS type, food contamination, label, and glue residuals.

Gel permeation chromatography

The molecular weight distribution (MWD) of virgin HIPS, and post-consumer HIPS samples (Group III), was determined by GPC according to the procedure previously reported by Lage-Rivera *et al*. [20]. The analysis was performed using a Waters Alliance 2695 separation module (Waters, Milford, MA, USA), equipped with a series of linear columns (Styragel HR 5E, Styragel HR 4E and Styragel HR3, 4.6 x 300 mm) and two detectors: a photodiode array detector (PDA, model 996 UV) and a refractive index detector (RI, model 2414). Analyses were carried out at 35 °C using tetrahydrofuran (THF) as the mobile phase at a flow rate of 0.3 mL min^{-1}. Polystyrene standards ranging from 580 to 3,080,000 Da were used for calibration (PDA at 220 nm). Dispersions of virgin and post-consumer HIPS (10 mg 8 mL^{-1} in THF) were stirred overnight, filtered (0.2 μm), and analyzed with RI-GPC. The data were used to inform MWD. The results (Mn: number-average mola mass, Mw: weight-average molar mass and Đ: polydispersity index) were reported as the average of three replicates and statical analysis was carried out using Statgraphics software. Significant differences in Mn, Mw and D values were analyzed by using one-way analysis of variance (ANOVA). $\alpha < 0.05$ of mean comparison was considered statistically significant.

Melt flow index

The melt flow index (MFI) of virgin and post-consumer HIPS was evaluated according to ASTM D1238 at 200 °C under a standard load of 5 kg. The analyses were done using a ZwickRoell melt flow tester (Mflow, Germany). Briefly, ~ 4 g of sample with a particle size 5 mm was preheated at 50°C for 5 min before testing. The mass of the extruded polymer was recorded and expressed in g 10 min^{-1}. Experiments were carried out in triplicate for each sample. Significant differences in MFI values of the same brand were analyzed by using Student's t-Test for Independent Samples. $\alpha < 0.05$ of mean comparison was considered statistically significant.

Thermogravimetric analysis (TGA)

Thermal stability of the materials was assessed by TGA using a TA Instruments Q50 analyzer (UE). Ground samples (~4 mg) were analyzed under a nitrogen atmosphere, with purge and balance gas flow rates of 40 and 60 mL min^{-1}, respectively. The samples were heated from 25 °C to 700 °C at a constant rate of 10 °C min^{-1}. The temperature and weight loss ranges in each decomposition step, as well as the residual mass percentage at 690 °C, were obtained from thermogravimetric/derivative thermogravimetric (TG/DTG) curves. The TGA measurements were carried out in duplicate (n = 2).

Differential scanning calorimetry (DSC)

Thermal transition analysis was performed using a PerkinElmer model 6000 differential scanning calorimetry equipment (UE) calibrated with indium standard (melting onset temperature = 156.6 ± 0.5 °C and fusion heat = 28.45 ± 1 J g^{-1}). Measurements were taken under a nitrogen atmosphere at a flow rate of 20 mL min^{-1}. Approximately 6 mg of the previously homogenized sample was weighed into 25 µL aluminum pans, which were then sealed. The temperature program consisted of an isothermal step at 25 °C for 1 min, then a heating from 25 to 200 °C at a heating rate of 10 °C min^{-1}. This was followed by an isothermal step at 200 °C for 5 min; then cooling from 200 °C to -50 °C at 10 °C min^{-1}; an isothermal step at -50 °C for 10 min, and finally, heating from -50 °C to 140 °C at 5 °C min^{-1}. The glass transition temperature (T_g) was determined at the second heating ramp. The analyses were performed in duplicate.

Metal quantification

The quantification of trace metal elements in post-consumer and virgin HIPS was carried out using ICP-MS (Thermo-Finnigan High Resolution Element XR). Previously, the samples were digested by microwave-assisted acid according to the method reported elsewhere [21].

To 0.1 g of previously homogenized post-consumer and virgin HIPS, 8 mL of 65% nitric acid, 2 mL of 30% hydrochloric acid, and 2 mL of 30% hydrogen peroxide were added. Digestion was performed in a microwave system (Ethos Easy, Milestone) following a five-stage program: (i) 5 min/1800 w at 120 °C, (ii) 15 min/1800 w at 180 °C, (iii) 15 min/1800 w at 220 °C, (iv) 15 min/1800 w at 220 °C, and (v) cooling for 45 min at room temperature. The resulting solutions were transferred to a 50 mL Erlenmeyer flask and made up to volume with ultrapure water and then filtered through 0.45 µm Millex HN membranes. ICP-MS equipment was operated at a plasma power of 1200–1400 W, with a nebulization gas flow of 0.8–1.0 L min^{-1}, an additional flow of 0.09–0.12 L min^{-1}, and a cooling gas flow of 15–16 L min^{-1}. A pneumatic nebulization system with a cyclonic chamber and nickel cones was used. Analyses were performed in dual mode (pulse counting and analogue mode) using internal standards of scandium-45, germanium-72, and indium-115 to account for interference and instrumental variations. Each sample was measured in triplicate runs in three consecutive passes, accumulating a total of nine readings per sample. Quantification was performed using external calibration via weighted linear regression.

Pyrolysis experiment

The grounded samples were pyrolyzed using a PyroProbe 5200 HPR (CDS Analytical, Oxford, PA, USA), which was coupled to a Clarus 690 GC (PerkinElmer, Cambridge, MA, USA) and connected to a Clarus SQ8T MS detector (PerkinElmer, Cambridge, MA, USA). The experiments were performed according to the protocol described elsewhere [22]. Briefly, each HIPS sample was loaded into a quartz pyrolysis tube containing approximately 50 mg of material and packed with quartz wool at both ends. The tube was placed within a Pt coil, and the samples were pyrolyzed at 550 °C, with a ramp rate of 12°C s^{-1} and a 15 s holding time in the heated zone after loading. The volatile pyrolysis products were trapped in a Tenax trap and then were heated at 280 °C and transferred to GC-MS using a heated transfer line (280 °C). The

volatile compounds were separated using an Elite 1701 capillary column (30 m × 0.25 mm × 0.25 μm) with high-purity helium at 15 mL min^{-1} as the carrier gas. The gas chromatograph oven was heated from 45 to 280 °C at a ramp rate of 4 °C min^{-1}. The volatile compounds were identified by comparing their mass spectra with those in the NIST 08 Mass Spectral Library. The spectral similarity criterion used was 90% or higher. Semi-quantitative determination of the volatile compounds was performed by calculating the peak areas in the chromatogram. In addition, the amount of the solid residue left in the pyrolytic tube consisted mainly of char formed by thermal cracking and was determined by direct weighing. The pyrolysis experiments were replicated at least twice, and the average result was reported.

Results and discussion

FTIR

ATR-FTIR spectroscopy was used to compare the spectral signatures of different parts of post-consumer yogurt cups from five dairy manufacturers, including Colun, Danone, Loncoleche, Nestlé, and Soprole. Figure 2 shows the average FTIR spectra of virgin and post-consumer HIPS. The post-consumer HIPS spectra were taken from three distinct areas of the aforementioned brands' cups: Fig. 2a corresponds to a clean external surface without label/adhesive residues; Fig. 2b corresponds to an internal food-contact surface; and Fig. 2c corresponds to an external surface with adhesive residues.

The FTIR spectra of the external and internal clean surfaces of post-consumer yogurt cups exhibited characteristic absorption bands of PS and PB, associated with the glassy and rubber phases, respectively. The main absorption bands of PS are at 696 and 753 cm^{-1}, which are associated with ring stretching and out-of-plane bending of the -CH- group in the aromatic ring of the styrene group, respectively [23]. The other bands of PS backbone features are: 1448 and 1491 cm^{-1} (aromatic skeleton stretching vibrations); 1601 cm^{-1} (C = C stretching); 2917 cm^{-1} (methylene stretching); 3003 cm^{-1} (aliphatic-chain C–H stretching associated with phenyl-substituted structures) and 3026 and 3058 cm^{-1} (aromatic C–H stretching) [24, 25]. On the other hand, PB in the HIPS sample is identified by the FTIR bands at 906 and 965 cm^{-1}, which are attributed to the out-of-plane bending of the C–H bonds of the vinyl-1,2 group and the trans-1,4 polybutadiene isomers, respectively [26]. However, the FTIR spectra collected from the internal food-contact surface (Fig. 3b) of some post-consumer cups displayed additional broad absorption bands around 1540,1640 cm^{-1}, and 1750 cm^{-1}, which may be associated with residual food contamination that was not removed by washing and cleaning. The band at 1750 cm^{-1}, which is associated with the C = O vibration, is a common feature of food waste, mainly from triglycerides and esterified fatty acids found in milk fat or the lipid fraction of yogurt [27]. The above-mentioned bands are mainly detected in the Soprole brand, indicating more yogurt residues after washing in this case.

The FTIR spectra of the yogurt cup surface with adhesive residues (Fig. 2c) differ from those taken from other parts of the cup, particularly in the regions between 750–1540 cm^{-1} and 2800–3000 cm^{-1}. In

general, the characteristic bands of HIPS are overlapped by those of the adhesive material. Food cups are commonly labelled using primarily adhesive-based resins such as ethylene-vinyl acetate copolymers, polyamides, polyesters, polyethylene and natural and synthetic rubber [28, 29]. The reduction in the intensities of the principal bands at 699 cm^{-1} and 966 cm^{-1} associated with PS and PB confirmed the presence of adhesive residues. The new bands clearly detected are: i) C-H asymmetrical vibration of CH_3 groups at 2955 cm^{-1}, which is attributed to hot-melt polyolefin adhesives, ii) C = O vibration of carbonyl groups at 1792 and 1737 cm^{-1} associated with anhydrides and ester groups, respectively, and indicates the presence of an ester resin tackifier, which improves adhesion between the paper label and plastic packaging [30], iii) CH_3 vibration at 1462 cm^{-1} associated with methyl and methylene groups of branched polyolefins and aliphatic tackifiers, iv) C-O vibration of ester groups at 1027 cm^{-1} in accordance with tackifier in the adhesive hot-melt [31, 32] v) stretching vibration of C–C in 3,4-unit at 1007 cm^{-1} and vi) out-of-plane bending vibration of CH_2 in the $–C=CH_2$ at 870 cm^{-1}. The above-mentioned suggests that residues correspond to polyolefin-based hot-melt with oxygenated tackifier resins, probably adhesive type amorphous polyalphaolefins with ester tackifier. These polyolefin-based adhesives with tackifiers are widely used in labels of yogurt cups and food packaging (Lommatzsch, Biedermann, Grob, & Simat, 2016).

PCA for FT-IR spectra

PCA was performed on the FTIR spectra of the three different surfaces of the yogurt cup from each commercial brand in the full spectrum region. This was used to identify samples of yogurt cups with similar chemical structures and to detect food waste contamination in post-consumer plastic. The first two principal components (PC)s accounted for 90%, with the first PC (PC1) and second (PC2) explaining 70.5 and 10.5%, respectively, of the spectral variation. Figure 3a illustrates the PCA biplots for PC1 vs.PC2 for the post-consumer samples (clean internal and external surfaces and adhesive residue surface) and the HIPS virgin. The analysis shows that there are two distinct clusters. One cluster is attributed to the adhesive residue surfaces with a negative PC1 score, and the other to the clean internal and external surfaces of the yogurt cups, located on the X-axis with lightly positive PC1 score. PC1 and PC2 dos not provided significative variations between the spectra of the clean internal and external container surfaces. This result indicates that the yogurt cup shared common chemical structure and minimal food contamination. In the loading plot of PC1 and PC2 (Fig. 3b), the signals observed in PC1 are those mainly attributable to adhesive residue. These bands with positive loading responsible for separating HIPS post-consumer samples along PC1 are 2955, 1400–1380 and 871 cm^{-1}. Other bands with strong negative loading are also observed in the PC1 loading at 752 and 699 cm^{-1}, which are associated to CH vibration of the aromatic ring of polystyrene.

A second PCA was conducted on the FTIR spectra to identify similarities in the adhesive residues from the yogurt cups. This PCA was performed in the fingerprint region (1630–400 cm^{-1}) of the FTIR spectra of the adhesive residue surfaces (Fig. 3c). The first two principal components accounted for 90% of the spectral variation, with PC1 and PC2 explaining 67.2% and 29.3%, respectively. The biplot of PC2 vs. PC1

shows that the adhesive residue surface from Soprole dairy manufacturing has a negative PC1 and PC2 quadrant, differentiating it from the other FTIR spectra. Additionally, the adhesives from the other commercial brands can be clustered together, suggesting that they share similar chemical nature. The PC1 and PC2 loading plot shows that the specific wavenumbers contributing to the scattering are 1409 and 1353 cm^{-1} (Fig. 3d). These broad absorption bands indicate the presence of C-O and free carbonyl groups in the adhesive residues [30].

MFI and molecular weight of polystyrene by GPC

Herein, the refractive index detector was used to report the MWD of the post-consumer HIPS samples. The Mn, Mw and Đ obtained from the GPC analyses are summarized in Table 1. The chromatograms detailing of the molecular weight of the samples versus elution time are shown in Online Resource 2. The Mn and Mw of the samples range from 87 to 105 kDa and from 228 to 282 kDa, respectively. Additional peaks can be observed in the chromatograms at elution times of 36.0 and 37.2 min, which are higher elution times than the peak for polystyrene. These peaks can be attributed to compounds of low molecular weight, which probably originate from the additives in the HIPS sample. Zinc stearate and Irganox 1076 [33] are additives commonly used in the formulation of HIPS. It is worth noting that the Mw and Mn of the Mix-GIII sample are approximately the average of the molecular weights of each of the samples, which is the expected result.

In general, as expected, post-consumer HIPS samples with a higher Mw had a lower MFI, and vice versa. The N-GIII sample with the highest Mw had the lowest MFI. Conversely, the C-GIII sample with the lowest Mw exhibited the highest MFI. However, this inverse correlation was not observed in all the post-consumer HIPS samples (L-GIII, S-GIII and D-GIII). Bremner et al. found a good correlation with Mark-Houwink's power law of the virgin polystyrenes of different ranges, where the inverse of the MFI values would be proportional to the average molecular weight raised to the power of 3.4[34]. Ferg & Bolo et al. [35] studied the relationship between MFI and Mw in virgin and recycled polypropylene, concluding that no effective correlation could be established between these two characteristics in recycled polymers. The factors such as fillers, impurities, and the presence of other polymers in the matrix can influence the polymer's flow properties.

Another relevant finding is that the MFI values of the adhesive residue-containing samples (Group II) are significatively higher than those of clean post-consumer samples (Group III), according to Student’s t-Test for Independent Samples and $\alpha < 0.05$. This finding suggests thermo-mechanical degradation induced by oxygenated adhesive residues, which led to chain scission of the polystyrene material during the MFI experiment, where heat and higher shear pressures are applied. The adhesive residues reduce the post-consumer HIPS´s stability, as will be demonstrated in the TGA results.

Table 1
Number average molecular weight (Mn), weight-average molecular weight (Mw), polydispersity index (Đ) and melt flow index (MFI) of virgin and post-consumer HIPS samples.

Sample code	Mn ($g\ mol^{-1}$)	Mw ($g\ mol^{-1}$)	Đ	MFI ($g\ 10\ min^{-1}$)
L-GII	-	-	-	5.0 ± 0.1
L-GIII	105000 ± 5000^{a}	258000 ± 9000^{ab}	2.46 ± 0.04^{ab}	3.3 ± 0.0^{a}
N-GII	-	-	-	3.2 ± 0.1
N-GIII	101000 ± 3000^{ab}	282000 ± 12000^{a}	2.80 ± 0.04^{bc}	2.8 ± 0.0^{b}
S-GII	-	-	-	3.9 ± 0.0
S-GIII	94000 ± 300^{abc}	251000 ± 9000^{bc}	2.67 ± 0.10^{abc}	3.6 ± 0.1^{c}
C-GII	-	-	-	5.3 ± 0.1
C-GIII	94000 ± 3000^{abc}	228000 ± 12000^{c}	2.42 ± 0.06^{a}	4.2 ± 0.1^{d}
D-GII	-	-	-	4.3 ± 0.0
D-GIII	87000 ± 5000^{c}	245000 ± 6000^{bc}	2.84 ± 0.21^{c}	3.2 ± 0.1^{e}
MIX-GIII	93000 ± 7000^{bc}	254000 ± 5000^{b}	2.75 ± 0.23^{abc}	3.50 ± 0.1
HIPS-V	99000 ± 2000^{ab}	241000 ± 3000^{bc}	2.43 ± 0.08^{ab}	5.1 ± 0.1^{ad}

Averages ± standard deviation of Mn, Mw and Đ calculated from 2 measurements; averages of MFI ± standard deviation calculated from 3 measurements. Superscript letter in the same column means the values are different statistically for α = 0.05 and Tukey HSD test.

TGA

Thermogravimetric analysis can be used to study the thermal decomposition of post-consumer and virgin HIPS. Figure 4 shows the thermogravimetric curves of post-consumer representative of clean samples (Group III), glue waste-containing samples (Group II) and label-containing samples (Group I), for Soprole samples, respectively. Similar weight loss behavior versus temperature was observed in the yogurt cups from other brands. The thermogravimetric curve of the virgin HIPS is shown in Fig. 4 to comparative purposes. In addition, Table 2 summarizes the temperature at which 1% mass loss occurs ($T_{1\%}$) temperature at which the maximum rate of decomposition (T_{max-}) and mass loss (Δm) occurs in each decomposition step, and the percentage of non-degraded residue at 690°C (Rm_{690}). In general, the post-consumer clean samples (Group III) and virgin HIPS display similar TGA curves (Fig. 4). According to the literature, HIPS thermal decomposition occurs in a single step between 350 and 500°C [5]. The

polymeric chains break down and evolve to the gaseous phase. However, the mass loss begins at about 180°C for virgin HIPS and 130°C for clean post-consumer HIPS (Group III), i.e., the samples start to decompose and release compounds before the onset of the unique decomposition step. In the revised literature, we don't find studies related to the continuous mass loss that occurs before 350°C. Vilaplana et al. [9] reported the presence of low molecular weight compounds in virgin and recycled HIPS by assessing them with microwave-assisted extraction and then followed by analysis of the extracts using GC–MS. Compounds formed by side reactions during the macromolecule polymerization, like styrene oligomers or monomer residues, were found as the main components. These compounds decompose before the polystyrene macromolecule, so the mass loss could be attributed to their decomposition or release from the polymer matrix. Additionally, the authors reported traces of aliphatic compounds, which were slightly higher in the recycled materials.

On the other hand, when comparing the temperatures at which 1 wt% mass loss occurs for virgin HIPS and clean post-consumer HIPS, a shift towards lower temperatures is observed, from 281°C for virgin HIPS to 214–235°C for Group III samples. Such decreases are representative of the fall in thermal stability resulting from the chain scission reaction during the first mechanical processing to elaborate the yogurt cups. The temperature at which the maximum decomposition rate occurs was slightly lower for the postconsumer samples of Group III (432 – 414°C) than for virgin HIPS (440°C). In general, the post-consumer samples have a higher residue content at 690°C than virgin material, which is related to the inorganic components present in the post-consumer cups and the carbon residue from the labels. The S-GIII and N-GIII samples showed the highest residue levels.

The values of $T_{1wt\%}$ for the adhesive residue-containing samples ranged from 180 to 210°C, which is lower than the values for clean post-consumer and virgin HIPS. Additionally, these samples exhibited a single decomposition step with T_{max-2} values around 430°C. The values of T_{max-2} and Δm_2 for adhesive residue-containing post-consumer HIPS ranged 176–210°C and 87.6–91.7%, respectively. The N-GII sample may be more sensitive to thermal degradation, with a lower T_{max-2}.

The TGA curves of the post-consumer, label-containing samples (Group I) show three degradation stages. The first stage is attributed to cellulose degradation (T_{max-1} ranged from 337 to 359°C) [36], the second to polystyrene degradation (T_{max-2} ranged from 423 to 440°C), and the third to char formation (T_{max-3} ranged from 629 to 656°C) [36]. These samples began to decompose as the temperature increased, with $T_{1wt\%}$ values between 40 and 60°C. The decomposition temperature of polystyrene shifts to a higher temperature compared to Group II and III samples. This can be attributed to the presence of char arising from the cellulose hindering depolymerization of the macroradicals in polystyrene [37].

In summary, the thermal stability of the samples, as evaluated by TGA, shows that the adhesive residue and the label itself decrease the stability of the post-consumer HIPS samples and contribute to the formation of stable carbon residues above 690°C. It is important to mention that the percentage of non-degraded residue showed deviation due to the inhomogeneity of the sample and the small weight measured in the TGA experiments.

Table 2
Thermal stability parameters determined by thermogravimetric analysisof virgin and post-consumer HIPS samples.

		1st decomposition step		2nd decomposition step		3rd decomposition step		
Sample	**$T_{1\%}$**	**T_{max-1}**	**Δm_1**	**T_{max-2}**	**Δm_2**	**T_{max-3}**	**Δm_3**	**$Rm_{690°C}$**
VPS	281	-	-	440.0	91.9	-	-	0.6
C-GI	42	348	25.5	436.0	40.8	629	8.0	11.2
C-GII	210	-	-	429.0	87.6	-	-	5.1
C-GIII	234	-	-	424.0	96.1	-	-	0.9
S-GI	55	359	26.4	440.0	41.7	636	5.4	16.9
S-GII	199	-	-	421.0	88.2	-	-	3.0
S-GIII	239	-	-	429.0	93.8	-	-	2.3
D-GI	35	354	25.5	428.0	48.4	638	6.2	7.2
D-GII	186	-	-	419.4	90.5	-	-	1.2
D-GIII	220	-	-	429.9	95.1	-	-	1.6
LL-GI	64	338	23.2	423.0	48.8	656	7.4	8.7
LL-GII	181	-	-	429.5	91.7	-	-	2.3
LL-GIII	232	-	-	424.6	96.7	-	-	0.2
N-GI	40	337	28.4	434.0	40.7	632	8.0	9.1
N-GII	176	-	-	425.5	90.7	-	-	2.3
N-GIII	214	-	-	433.2	92.8	-	-	3.2

$T_{1\%}$ corresponds to the temperature at which 1% mass loss occurs, T_{max} to the temperature at which the maximum rate of decomposition occurs, Δm to mass loss in each decomposition step, and to $R_{m690°C}$ the residual mass at 690°C. The 1, 2 and 3 subscripts of T_{max} and Δm refer to the first, second and third decomposition stages, respectively.

DSC

Figure 5 shows the DSC first and second heating of virgin and postconsumer HIPS samples. A clear endothermic peak is observed during the first heating scan of the adhesive residue-containing samples (Group II). This thermal transition at around 60°C probably corresponds to the tackifier's relaxation

during heating of the adhesive resin formulation. The reported relaxation structure temperature during the first heating run for tackifier of chemical nature such as ester and polyterpene resins is around 60°C[31]. The adhesive residue-containing sample from Soprole cups exhibited higher T_m values than the other GII group samples. This finding provides further evidence of the adhesive chemical difference in these samples, as demonstrated by the FTIR analyses.

After the thermal history is erased (i.e., in the second heating scan), this endothermic peak can no longer be observed. In addition, there are no significant changes in the T_g values of the first heating scan of the virgin and postconsumer samples. The average T_g values fluctuated between 96 and 101°C. However, a fall in the glass transition temperature of the adhesive-containing samples in the second heating scan is clearly observed. The decrease of the T_g values of adhesive-containing (Group II) samples oscillated between 6 and 12°C in comparison to the T_g values of clean post-consumer (Group III) samples of the same brand (see Table 3). A significant widening of the glass transition region of the adhesive-containing samples is also observed (Fig. 5c). In general, samples with higher label content and therefore higher adhesive residues exhibited greater differences in glass transition temperature between the first and second scans. Thus, the decrease was 12.8°C for C-GII (26% label), 11.4°C for D-GII (20% label), 6.6°C for L-GII (18% label), 6.8°C for S-GII (17% label), and 8.4°C for N-GII (14% label). The latter result was greater than expected, indicating a greater amount of glue adhering to the Nestlé brand packaging, or a certain heterogeneity in the recycled samples. The T_g values of M-GII and M-GIII samples differed by 9.2°C in the second heating scan, which is equivalent to the mean of the five brands of yogurt cups. The changes observed in the glass transition of the PS phase in post-consumer HIPS samples with and without adhesive are probably the result of thermal-degradation reactions that take place during the first heating. These results are consistent with the increase in MFI of the Group II samples compared to Group III samples, as well as the TGA results. The dependence of the T_g values of polystyrene on molecular weight is well established by several authors [38, 39]. Based on these findings, it can be concluded that the reduction in the glass transition temperature of adhesive residue-containing yogurt cups (Group II sample) could be mainly related to two factor: i) the decrease in molecular weight as a result of the degradation taking place in HIPS matrix when heated to 200°C in the presence of adhesive residues and ii) adhesive residues with a lower molecular weight act as free molecules, creating more space between polymer chains and reducing the glass transition temperature

Table 3
Thermal transition parameters of virgin HIPS and postconsumer HIPS (clean and adhesive residue-containing) samples determined by differential scanning calorimetry.

Sample	T_{m1}	T_{g1} (°C)	T_{g2} (°C)
PS-V	-	96 ± 4.0	92 ± 1.0
L-GII	58 ± 2.0	98 ± 1.0	85 ± 2.0
L-GIII	-	101 ± 3.0	93 ± 4.0
N-GII	58 ± 1.0	98 ± 0.7	84 ± 1.0
N-GIII	-	101 ± 1.0	92 ± 0.2
S-GII	60 ± 0.2	97 ± 0.1	85 ± 2.0
S-GIII	-	99 ± 2.0	92 ± 2.0
C-GII	59 ± 2.0	96 ± 3.0	82 ± 0.5
C-GIII	-	101 ± 3.0	93 ± 4.0
D-GII	57 ± 1.0	97 ± 1.0	82 ± 0.5
D-GIII	-	96 ± 2.0	93 ± 1.0
MIX-GIII	-	98 ± 0.1	92 ± 0.2

T_g and T_m values were determined by DSC at 10°C min^{-1}. The 1 and 2 subscripts of T_g and T_m refer to the first and second heating scan, respectively.

ICP-MS

Inorganic substances present in post-consumer plastics can be added intentionally or unintentionally. For example, metal oxides (e.g. Sb, Ti, Cr, Hg, Mn) are intentionally added during the production of plastic as catalysts. Similarly, additives such as colorants containing metals (e.g. Ti, Cr, Co, Cd, Pb, Zn, Fe, Al, Cu), antioxidants and stabilizers (e.g. Cd, Pb, Zn) or other additives containing metals and metalloids (e.g. Li, Pb, Cd, Zn, Sb, Al) are added to the plastic formulation [21].

Figure 6 illustrates the concentrations of Al, Fe, Ti and Zn divided according to the yogurt commercial brand of the label-containing samples (Group I), using a bar graph. Figure 6 also includes the mixed groups defined in this study for adhesive residue-containing samples (MIX-GII) and post-consumer clean samples (MIX-GIII), as well as virgin HIPS. The concentrations of metals and metalloids such as As, Cd, Co, Sb and Hg were below the detection limit of the equipment: <0.25, < 0.25, < 0.25, < 1.25 and < 0.01, respectively. Additionally, the metal concentration in post-consumer HIPS samples was higher than in

virgin HIPS. The Al, Cr and Fe concentrations of the post-consumer samples decreased in the following order: GI > MIX-GII > MIX-GIII.

The samples containing labels exhibited an Al concentration ranging from 1,090 to 3,800 μg g^{-1}, an Fe concentration ranging from 7.7 μg g^{-1} to 270, a Ti concentration 0.72 to 353 μg g^{-1} and a Cr concentration ranging from 4 to 0.95 μg g^{-1}. The Al concentration was considerably higher in the label-containing samples than in the adhesive-containing and clean samples. Aluminum ($Al_2(SO_4)_3 \cdot 18H_2O$) is used as a sizing agent in papermaking to slow the rate at which liquids (water, ink, etc.) penetrate the paper structure [40]. The samples with a higher percentage of the label, C-GI and D-GI, had a higher Al concentration. The N-GI sample with the lowest label percentage had the lowest Al concentration. Aluminum was also the most prevalent metal in the adhesive-containing samples; however, its concentration decreased by more than 50% compared to the concentration of aluminum in the label-containing samples. This could be related to aluminum sulfate residue from the labels.

The relevant finding was that the Zn concentration, which ranged between 50 and 116 μg g^{-1}, did not provide from the label or adhesive. The Zn concentration was within the same order of magnitude as reported in post-consumer polystyrene samples (50–120 μg g^{-1}) by Eriksen et al. [21] Zn compounds result from the intentional addition of Zn-containing additives during HIPS transformation for example in the form of Zn stearate, used as lubricant during the production stage of the yogurt cups.

Chemical recycling

In general, the main depolymerization mechanisms during polymer pyrolysis are: (i) unzipping, which involves repeated and successive C-C scission; (ii) back-biting, which is produced by intramolecular hydrogen transfer followed by mid-chain carbon bond scission and leads to low molecular weight compounds; and (iii) random scission, where intramolecular hydrogen transfer is followed by β-scission, providing a great variety of low molecular weight products [1]. In the case of HIPS´ pyrolysis, the main mechanism, as mentioned above in the introduction, is unzipping reaction.

First, the char residue of HIPS pyrolysis samples was around 0.2 wt.%, and this percentage did not depend on the cellulose and adhesive content or the brand cups. This confirms that the pyrolysis of post-consumer yogurt cups offers promising results if the aim is to produce valuable gaseous fractions. In addition, the obtained char percentages are in accordance with those reported in previous similar studies employing a fixed bed tubular reactor [41] or a wire-mesh reactor [42], but lower than that of HIPS pyrolysis at 515°C in a fluidized bed reactor (11 wt.%) [43]. Differences are associated with pyrolysis reactor type and experimental conditions.

Figure 7 summarizes the family product distributions and the five majority compound distributions of the aromatic hydrocarbon fraction resulting from the thermo-pyrolysis of post-consumer and virgin HIPS. The aliphatic hydrocarbon fraction accounted for less than 3% of the total, and 4-ethenyl-cyclohexene was the predominant compound in almost all pyrolyzed samples. This compound has also been

identified in the pyrolysis of styrene-butadiene rubber, albeit not as a major component [44]. Reports on the pyrolysis of HIPS indicate that 1,3-butadiene is one of the most abundant pyrolyzates within the aliphatic hydrocarbon fraction [45]. However, it was not detected in the pyrolyzed HIPS samples.

In general, a great variety of low molecular weight aromatic pyrolyzates were obtained from samples containing labels (Group I), compared with Group II and III samples. Nallar & Wong et al. [46] reported that cellulose promotes the production of low-molecular-weight compounds in polystyrene, as well as polystyrene hinders the production of levoglucosan. They propose that the inhibitory effect on the cleavage of glycosidic bonds in anhydro sugar oligomers in cellulose is caused by the aromatic groups in polystyrene. Sugar pyrolyzates were not detected in this study. In addition, oxygenated hydrocarbons, such as acids, alcohols, esters and aldehydes, only appeared in the pyrolysis product stream of Group I samples, which contain oxygen-bearing polymers such as cellulose [37]. The relative content of oxygenated compounds was 0.32%, 2.70%, 0.12%, 2.38% and 4.54% for D-GI, C-GI, N-GI, S-GI and L-GI, respectively. No correlation could be established between the label content and oxygenated pyrolysis products. A plausible explanation for the lacks of correlation would be the small amount of pyrolyzed samples (50 mg), which makes it difficult to ascertain the exact label-plastic ratio.

As expected, the aromatic hydrocarbon fraction predominates in the pyrolysis of HIPS (65–86% relative area). The main degradation product detected by pyrolysis–gas chromatography was styrene monomer, followed by toluene and α-methylstyrene [1]. Other pyrolysis products were successfully identified in the post-consumer HIPS pyrograms, with a relative area percentage ranging from 0.3 to 3%. These included alkylbenzene, benzene, indene, naphthalene, 1,2-dihydro-naphthalene, cyclopropylphenylmethane, bibenzyl and (1-methylenebutyl)-biphenyl (Online Resource 3). Not all of the compounds mentioned above were found in all of the samples, and in some cases their relative percentage was less than 0.3%. Furthermore, diphenylmethane, a dimer, was present in C-GI, N-GI and S-GII samples, but only at levels of 0.2% or lower.

The yield of styrene in the non-catalytic pyrolysis of samples from Group I was lower than that of Groups II and III (see Figs. 7b, c and d). The styrene monomer yield was 59–88% for label containing samples (Group I), 64–94% for glue containing residues samples (Group II), and 81–94% for clean samples (Group III). A relevant aspect of the present work is that the uncatalyzed pyrolysis of post-consumer HIPS yields a higher styrene monomer content than virgin HIPS, taking as reference material. The styrene yield of virgin HIPS was only 73%. Additionally, the styrene yields obtained in the non-catalytic pyrolysis of post-consumer HIPS was higher than those reported in several research studies. Inayat et al. [11] studied the non-catalytic pyrolysis of post-consumer HIPS from the recycling of cups used for dairy products at 500°C, finding a styrene content of around 60% in the pyrolysis oil. In this case, the styrene yield of virgin HIPS was superior at the same pyrolysis condition, at around 65%. Giakoumakis et al. [33] studied the thermolysis of HIPS in a pyrolysis reactor at 300°C (heating rate: 2.5°C.min^{-1}) under a continuous nitrogen flow and reported a styrene yield in the liquid phase of 49%. Similar results were found Monteiro et al. for pyrolysis of HIPS using a tubular quartz laboratory-scale reactor at 500°C with continuous nitrogen flow [47]. The authors propose that the low selectivity in the production of styrene is

due to the presence of PB particles that contribute to the formation of stable tertiary radicals in the backbone of the grafted PS. These radicals then end up producing toluene, ethylbenzene and α-methylstyrene, preferentially.

Here, the formation of comparatively higher amounts of styrene monomer in the case of the group III sample compared to virgin HIPS may be ascribed to its lower polybutadiene content compared to virgin HIPS, and to the presence of metal and metal oxides incorporated into the formulation of the HIPS containers for dairy products, such as Ti, Al, Fe and Zn. According to the results of the ICP-MS analysis, these metals are present in large quantities in post-consumer HIPS. Guoxi et al. [48] have reported on the effects of Al, Zn, Fe, Ni, and Cu powders on the thermal degradation of waste polystyrene (ratio 10:1, polymer : metal). The results show that the metals increased the yield of styrene monomer. In particular, aluminum showed the greatest selectivity of the five metals studied for styrene monomer conversion. The authors suggested that polystyrene degrades through a transient intermediate in the presence of metal powders. First, radicals form transient intermediates with the metals, and second, these intermediates degrade to produce styrene monomer. When the electronegativity of the metal is lower, the forces between the metals and radicals in transient intermediates are weaker, and therefore the second step is the determining reaction in polystyrene degradation.

In addition, metal oxides such as TiO_2, which is used as a pigment to provide plastics with whiteness and high opacity, are incorporated into the formulation of HIPS cups for dairy products. TiO_2 also exhibits Lewis acidity and has a large surface area and non-toxic sites, which are useful for the catalytic cracking of several plastics. Nwankwor et al. [49] have shown that TiO_2 acts as a catalyst in the pyrolysis of PS waste, increasing the liquid fraction and the selectivity of styrene compared to PS that has not been treated with a catalyst. Overall, we have demonstrated the significant potential for producing styrene from waste plastics through non-catalytic cracking of post-consumer HIPS from food packaging. Furthermore, we have shown that the production of this monomer is more selective when the labels and adhesives present on the packaging are efficiently removed.

Conclusion

Post-consumer HIPS from yogurt cups sold in Chile is a promising waste resource for producing value-added products through non-catalytic pyrolysis. The homogeneity of the chemical composition of post-consumer HIPS, as well as the minimal food contamination, are significant advantages of this feedstock for chemical recycling process. Additionally, the presence of contaminating metals, such as titanium (Ti) and aluminum (Al), promotes the production of aromatic compounds, mainly styrene, even when paper and adhesive residues are present in the plastic waste.

Declarations

Acknowledgement

This work was funded by Agencia Nacional de Investigación y Desarrollo (ANID) through of grant projects: ANID Regional R23F0005, FONDECYT 1261207, CIA250002 and CTI 25000.

Statements and declarations

Competing interests: The authors declare that they don´t have competing interests

CRediT authorship contribution statement

Saddys Rodríguez-Llamazares: Writing – Original Draft; Conceptualization; Investigation; Funding acquisition.

Mario I. Sanhueza: Supervision; Data Curation; Methodology.

Constanza Sabando: Methodology; Investigation.

Diego Ricciardi: Investigation; Methodology.

Serguei Alejandro-Martín: Conceptualization, Investigation.

Rebeca Bouza: Investigation; Methodology.

Sonia Dopico: Methodology.

Natalia Pettinelli: Investigation.

Edgar Pastene: Methodology, Investigation.

Eliezer Velásquez: Writing – Review & Editing**.**

Declaration of generative AI and AI-assisted technologies in the writing process

During the preparation of this work, the authors used DeepL to correct spelling and grammatical errors. After using this tool/service, they reviewed and edited the content as needed and assume full responsibility for the content of the publication.

Data availability

Data will be made available on request.

References

1. Lei, H., et al., *Recent advancements in the chemical recycling and biodegradation of post-consumer polystyrene waste.* Green Chemistry, 2025. **27**(31): p. 9357-9413.
2. zu Castell-Rüdenhausen, M., *Material flow analysis and modelling of the feedstock potential for recycling polystyrene.* Circular Economy, 2025. **4**(1): p. 100127.

3. Subbaiah, Y., et al., *Influence of submicron tiny gel rubber particles on the estimation of grafting and rubber efficiency in high-impact polystyrene.* Journal of Elastomers and Plastics, 2017. **49**: p. 684-695.
4. Velásquez, E., et al., *Partitioning of the components into two-demixed-macrophases from a solution blend emulating high impact polystyrene close to the phase inversion region.* Polymer, 2020. **198**: p. 122523.
5. Velásquez, E., et al., *Repetitive mechanical recycling of post-consumer high impact polystyrene from yogurt cups: A pilot-scale performance assessment at different reprocessing cycles.* Resources, Conservation and Recycling, 2024. **202**: p. 107368.
6. Lacoste, J., et al., *Polybutadiene content and microstructure in high impact polystyrene.* Journal of Applied Polymer Science, 1996. **59**: p. 953-959.
7. Soriano, F. and R. Díaz de León, *Recycling of high impact polystyrene in coextruded sheet: Influence of the number of processing cycles on the microstructure and macroscopic properties.* Polymer Engineering & Science, 2006. **46**: p. 1698-1705.
8. Belblidia, F., et al., *Recycling high impact polystyrene: Material properties and reprocessing in a circular economy business model.* Progress in Rubber, Plastics and Recycling Technology, 2023. **39**(4): p. 343-363.
9. Vilaplana, F., A. Ribes-Greus, and S. Karlsson, *Analytical strategies for the quality assessment of recycled high-impact polystyrene: A combination of thermal analysis, vibrational spectroscopy, and chromatography.* Analytica Chimica Acta, 2007. **604**(1): p. 18-28.
10. Calero, M., et al., *Oil and gas production from the pyrolytic transformation of recycled plastic waste: An integral study by polymer families.* Chemical Engineering Science, 2023. **271**.
11. Inayat, A., et al., *Chemical recycling of waste polystyrene by thermo-catalytic pyrolysis: A description for different feedstocks, catalysts and operation modes.* Polymer Degradation and Stability, 2022. **201**: p. 109981.
12. Liu, J., et al., *Catalytic effect and mechanism of in-situ metals on pyrolysis of FR4 printed circuit boards: Insights from kinetics and products.* Chemosphere, 2021. **280**: p. 130804.
13. Ainali, N.M., D.N. Bikiaris, and D.A. Lambropoulou, *Aging effects on low- and high-density polyethylene, polypropylene and polystyrene under UV irradiation: An insight into decomposition mechanism by Py-GC/MS for microplastic analysis.* Journal of Analytical and Applied Pyrolysis, 2021. **158**: p. 105207.
14. Seeley, M.E. and J.M. Lynch, *Previous successes and untapped potential of pyrolysis–GC/MS for the analysis of plastic pollution.* Analytical and Bioanalytical Chemistry, 2023. **415**(15): p. 2873-2890.
15. Déparrois, N., et al., *Syngas production from co-pyrolysis and co-gasification of polystyrene and paper with CO2.* Applied Energy, 2019. **246**: p. 1-10.
16. Anshu, K., H.I. Kenttämaa, and S.K. Thengane, *A comprehensive review on co-pyrolysis of lignocellulosic biomass and polystyrene.* Renewable and Sustainable Energy Reviews, 2024. **205**: p. 114832.

17. Baena-González, J., et al., *Chemical recycling of plastic waste: Bitumen, solvents, and polystyrene from pyrolysis oil.* Waste management, 2020. **118**: p. 139-149.
18. Andriotis, E.G. and D.S. Achilias, *Role of Polylimonene as a Bio-Based Additive in Thermal Oxidation of High Impact Polystyrene.* Macromolecular Symposia, 2013. **331-332**(1): p. 173-180.
19. Campagna, R., C. Conti, and S. Cuomo, *Smoothing exponential-polynomial splines for multiexponential decay data.* Dolomites Research Notes on Approximation, 2020. **12**: p. 86-100.
20. Lage-Rivera, S., et al., *Comparing lignin and spent coffee grounds as bio-fillers in PLA 3D-printable filaments.* Polymer Composites, 2024. **45**(16): p. 14566-14579.
21. Eriksen, M.K., et al., *Contamination in plastic recycling: Influence of metals on the quality of reprocessed plastic.* Waste Management, 2018. **79**: p. 595-606.
22. Romero-Unda, C., B. Puentes-Navarro, and S. Alejandro-Martín, *Dataset on the analytical cohydropyrolysis of chilean oak and polyethylene under catalytic and noncatalytic conditions.* Data in Brief, 2025. **63**: p. 112134.
23. Sekhar, V.C., et al., *Microbial degradation of high impact polystyrene (HIPS), an e-plastic with decabromodiphenyl oxide and antimony trioxide.* Journal of Hazardous Materials, 2016. **318**: p. 347-354.
24. Vilaplana, F., A. Ribes-Greus, and S. Karlsson, *Degradation of recycled high-impact polystyrene. Simulation by reprocessing and thermo-oxidation.* Polymer Degradation and Stability, 2006. **91**(9): p. 2163-2170.
25. Zhang, J., et al., *Compatibility of waste rubber powder/polystyrene blends by the addition of styrene grafted styrene butadiene rubber copolymer: effect on morphology and properties.* Polymer Bulletin, 2013. **70**: p. 2829-2841.
26. Zhang, S., et al., *Deformation and toughening mechanism for high impact polystyrene (HIPS) by pressure-induced-flow processing.* RSC Advances, 2013. **3**(19): p. 6879-6887.
27. Cantero-Tubilla, B., et al., *Characterization of the solid products from hydrothermal liquefaction of waste feedstocks from food and agricultural industries.* Journal of Supercritical Fluids, 2017. **133**: p. 665-673.
28. Sanghvi, M., O. Tambare, and A. More, *Performance of various fillers in adhesives applications: a review.* Polymer Bulletin, 2022. **79**: p. 1-63.
29. Chugh, K., G. Phalak, and S.T. Mhaske, *Preparation and characterization of a polyester-etheramide hot melt adhesive system from renewable resources.* International Journal of Adhesion and Adhesives, 2019. **95**: p. 102432.
30. Larkin, P., *Infrared and Raman Spectroscopy; Principles and Spectral Interpretation*. 2011.
31. Barrueso-Martínez, M.L., et al., *Influence of the vinyl acetate content and the tackifier nature on the rheological, thermal, and adhesion properties of EVA adhesives.* Journal of Adhesion Science and Technology, 2001. **15**(2): p. 243-263.

32. Yuan, B., C. McGlinchey, and E.M. Pearce, *Explanation of tackifier effect on the viscoelastic properties of polyolefin-based pressure sensitive adhesives.* Journal of Applied Polymer Science, 2006. **99**(5): p. 2408-2413.
33. Giakoumakis, N.S., et al., *Total revalorization of high impact polystyrene (HIPS): enhancing styrene recovery and upcycling of the rubber phase.* Green Chemistry, 2024. **26**(1): p. 340-352.
34. Bremner, T., A. Rudin, and D.G. Cook, *Melt flow index values and molecular weight distributions of commercial thermoplastics.* Journal of Applied Polymer Science, 1990. **41**(7-8): p. 1617-1627.
35. Ferg, E.E. and L.L. Bolo, *A correlation between the variable melt flow index and the molecular mass distribution of virgin and recycled polypropylene used in the manufacturing of battery cases.* Polymer Testing, 2013. **32**(8): p. 1452-1459.
36. Mishra, R.K., et al., *Pyrolysis of waste pinewood sawdust using Py-GC-MS: effect of temperature and catalysts on the pyrolytic product composition.* RSC Sustainability, 2025. **3**(11): p. 5314-5325.
37. Jakab, E., M. Blazso, and O. Faix, *Thermal decomposition of mixtures of vinyl polymers and lignocellulosic materials.* Journal of Analytical and Applied Pyrolysis - J ANAL APPL PYROL, 2001. **58**: p. 49-62.
38. Arraez, F., M. Arnal, and A. Müller, *Thermal degradation of high-impact polystyrene with pro-oxidant additives.* Polymer Bulletin, 2019. **76**.
39. Peterson, G., et al., *Mechanochemical Degradation of Amorphous Polymers with Ball-Mill Grinding: Influence of the Glass Transition Temperature.* Macromolecules, 2020. **53**: p. 7795-7802.
40. Jablonsky, M., J. Šima, and M. Lelovsky, *Considerations on factors influencing the degradation of cellulose in alum-rosin sized paper.* Carbohydrate Polymers, 2020. **245**: p. 116534.
41. Antonakou, E.V., et al., *Pyrolysis and catalytic pyrolysis as a recycling method of waste CDs originating from polycarbonate and HIPS.* Waste Management, 2014. **34**(12): p. 2487-2493.
42. Zhou, J., et al., *Formation of styrene monomer, dimer and trimer in the primary volatiles produced from polystyrene pyrolysis in a wire-mesh reactor.* Fuel, 2016. **182**: p. 333-339.
43. Jung, S.-H., S.-J. Kim, and J.-S. Kim, *The influence of reaction parameters on characteristics of pyrolysis oils from waste high impact polystyrene and acrylonitrile–butadiene–styrene using a fluidized bed reactor.* Fuel Processing Technology, 2013. **116**: p. 123-129.
44. Lou, J.C., G.F. Lee, and K.S. Chen, *Incineration of styrene–butadiene rubber: the influence of heating rate and oxygen content on gas products formation1Revised manuscript submitted for publication in J. Hazard. Mater.—Issue on Waste Management Technology, Taiwan, China.1.* Journal of Hazardous Materials, 1998. **58**(1): p. 165-178.
45. Charitopoulou, M.A., A.A. Lappas, and D.S. Achilias, *Thermo-chemical recycling of plastics retrieved from waste electric and electronic equipment (WEEE) by pyrolysis: Identification of the polymer type, removal of bromine compounds from plastics based on an environmentally-friendly process and characterization of the pyrolysates.* Sustainable Chemistry and Pharmacy, 2023. **35**: p. 101210.
46. Nallar, M. and H.-W. Wong, *Hydroxyl Group Stabilization for Increased Yields of Low-Molecular-Weight Products in the Copyrolysis of Cellulose and Thermoplastics.* Industrial & Engineering Chemistry

Research, 2019. **58**: p. 10776-10784.

47. Monteiro, A., et al., *Life Cycle Assessment of the Catalytic Pyrolysis of High-Density Polyethylene (HDPE) and High-Impact Polystyrene (HIPS).* Macromolecular Reaction Engineering, 2022. **16**: p. 2200037.
48. Guoxi, X., et al., *Mechanism studies on the catalytic degradation of waste polystyrene into styrene in the presence of metal powders.* Journal of Applied Polymer Science, 1999. **73**(7): p. 1139-1143.
49. Nwankwor, P., et al., *Synthesis of gasoline range fuels by the catalytic cracking of waste plastics using titanium dioxide and zeolite.* International Journal of Energy and Environmental Engineering, 2020. **11**: p. in press.

Figures

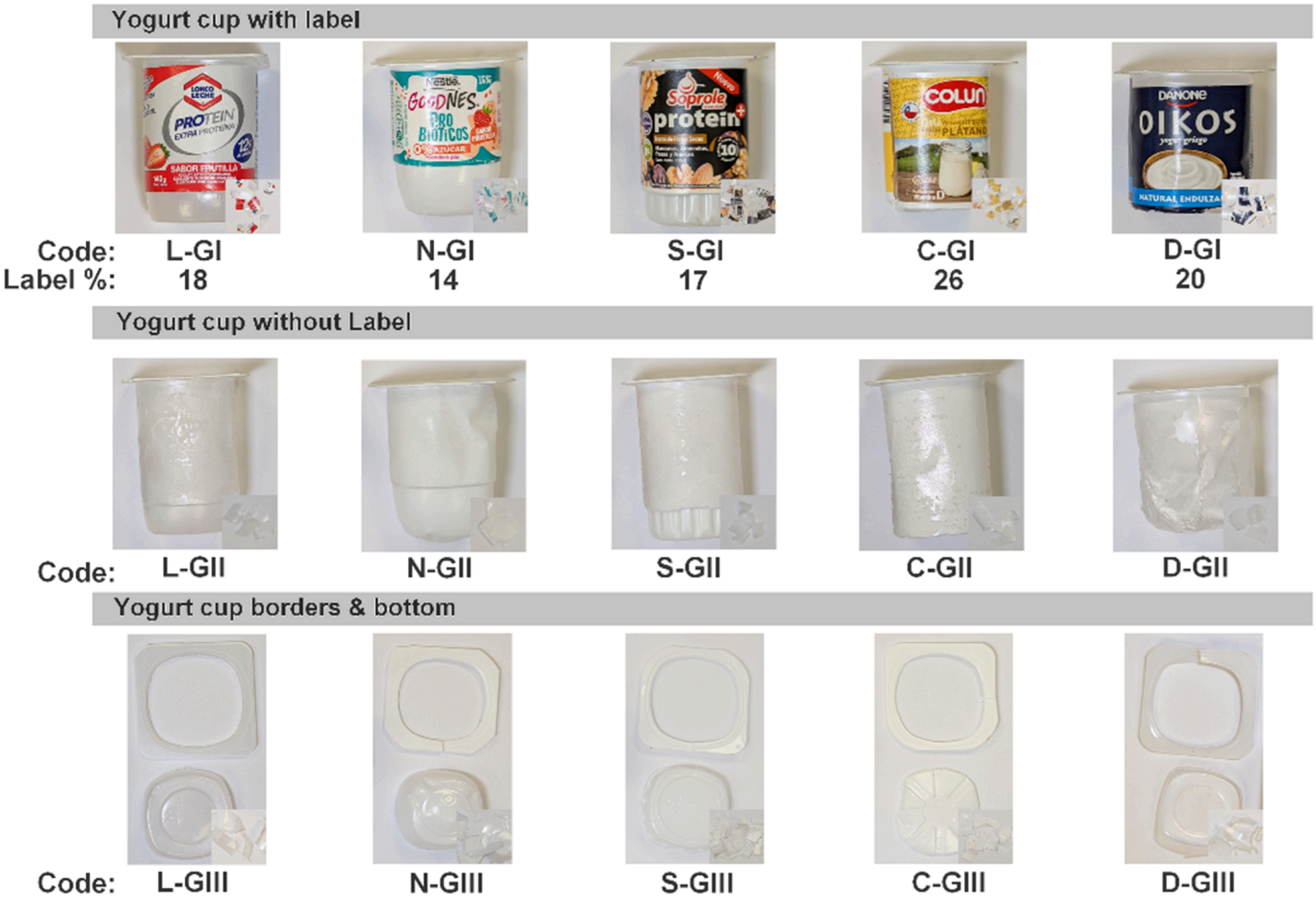


Figure 1

Photographs of post-consumer yogurt cups. The sample codes and percentage labels for each brand cup are also illustrated. L, N, S, C, and D refer to the Loncoleche, Nestlé, Soprole, Colun and Danone brands, respectively. GI, GII, and GIII correspond to the group number, respectively. The insert in the top right-hand of each picture shows the grounded material.

Before homogenization, the percentage of label on the cups of each yogurt brand was determined by gravimetry, considering the mass of the whole yogurt cup with label (Group I) and after removing it (Group II). The samples, separated by brand and group, were cut by hand and then cryogenically ground using an IKA A11 Basic blade mill. The samples were sieved, and the fraction smaller than 425 µm was used for further analysis.

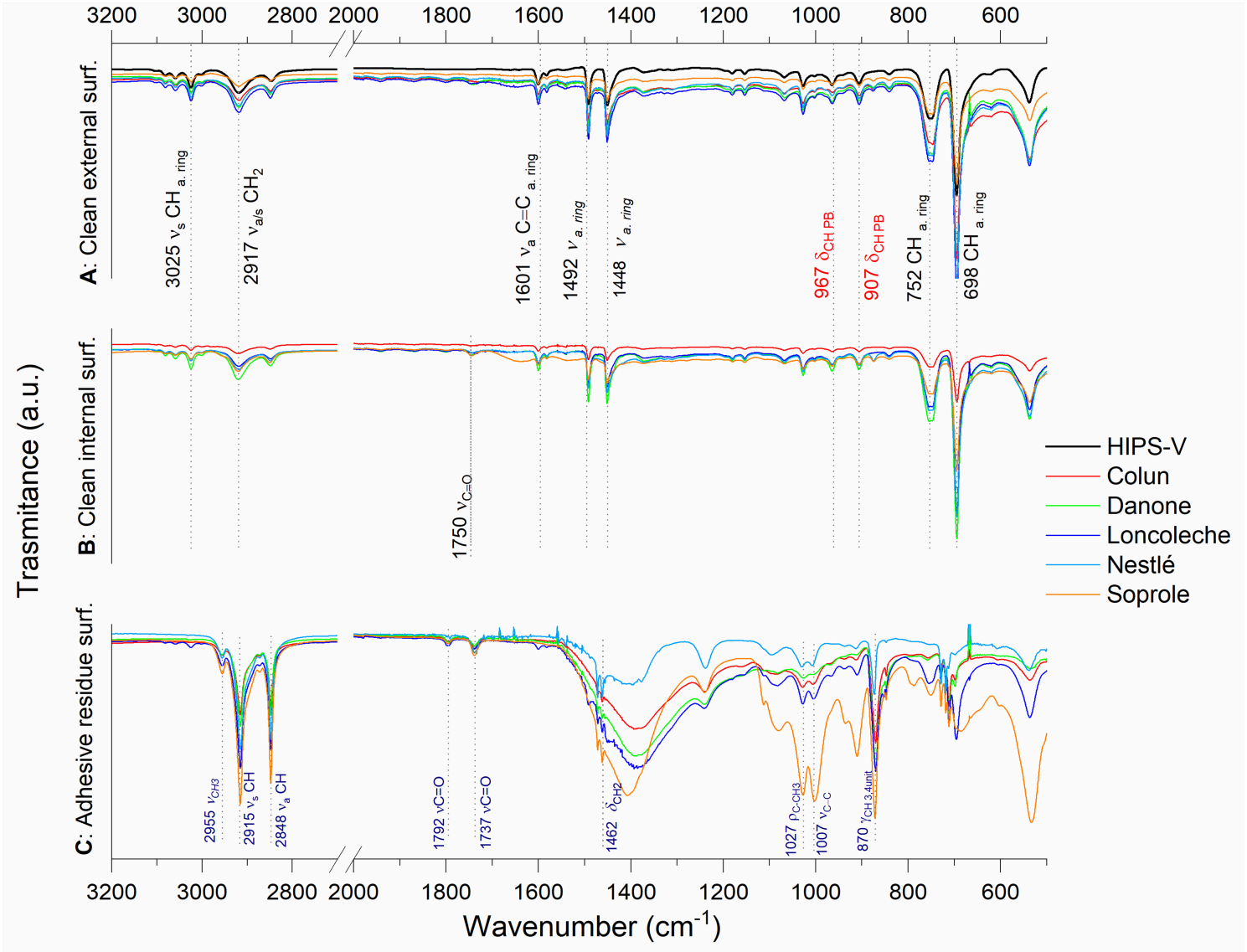


Figure 2

FTIR spectra of different parts of post-consumer yogurt cups from five dairy manufacturers, including Colun, Danone, Loncoleche, Nestlé, and Soprole. a: corresponds to a clean external surface without

label/adhesive residues; b: to an internal food-contact surface; and c: external surface with adhesive residues.

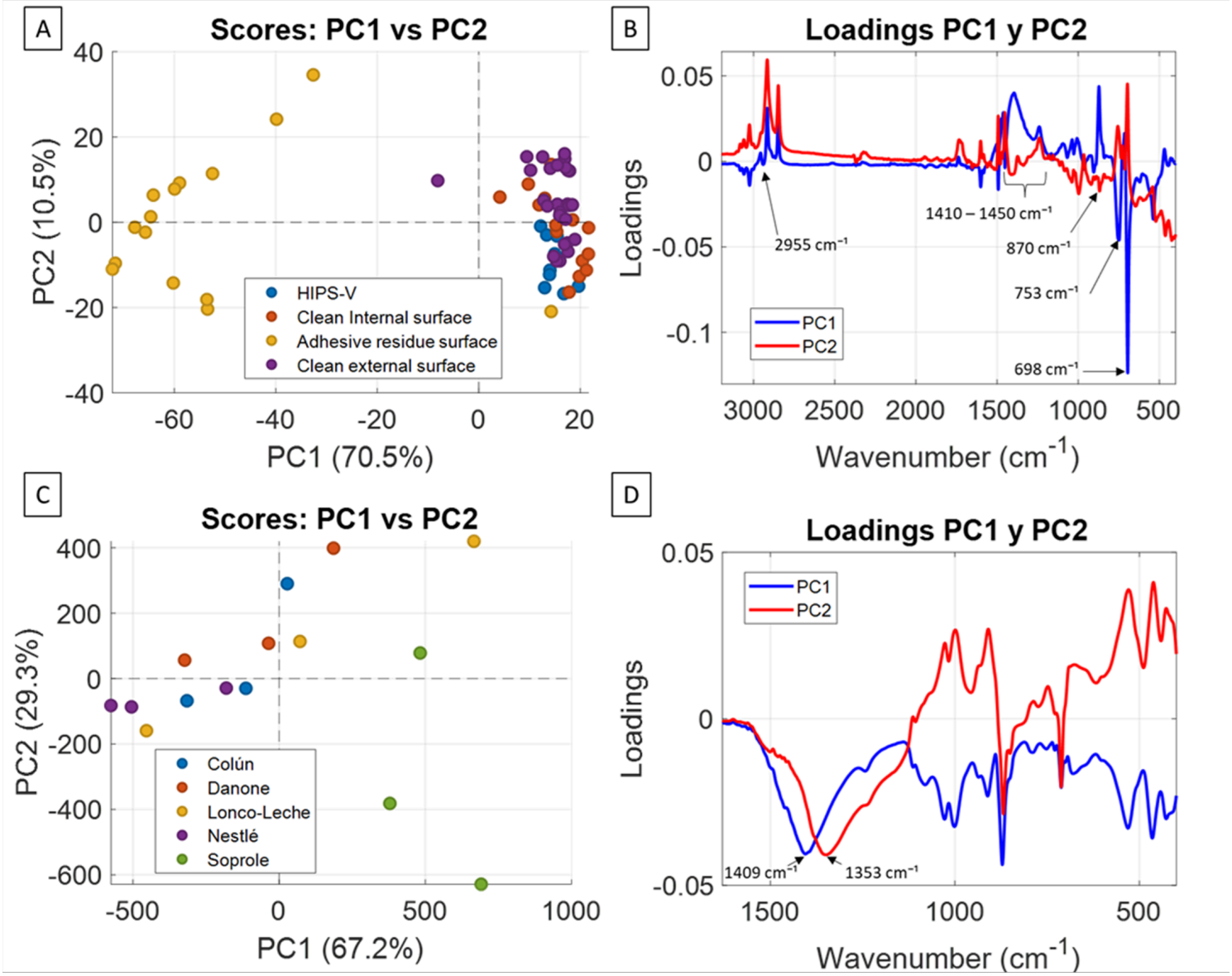


Figure 3

Principal component analysis (PCA) for FTIR spectra of different parts of post-consumer yogurt cups from several dairy manufacturers: (a) bi-plot for all FTIR spectra showing the common chemical structure and minimal food contamination of HIPS postconsumer cups; (b) loading plot of PC1 and PC2 vs. FTIR wavenumber showing the specific wavenumbers that contributed to the scattering between all samples; (c) biplot for FTIR spectra of the adhesive residue surface of the cups in the 1600-400 cm^{-1} region and (d) loading plot of PC1 and PC2 vs. FTIR wavenumber showing differences between adhesive residues.

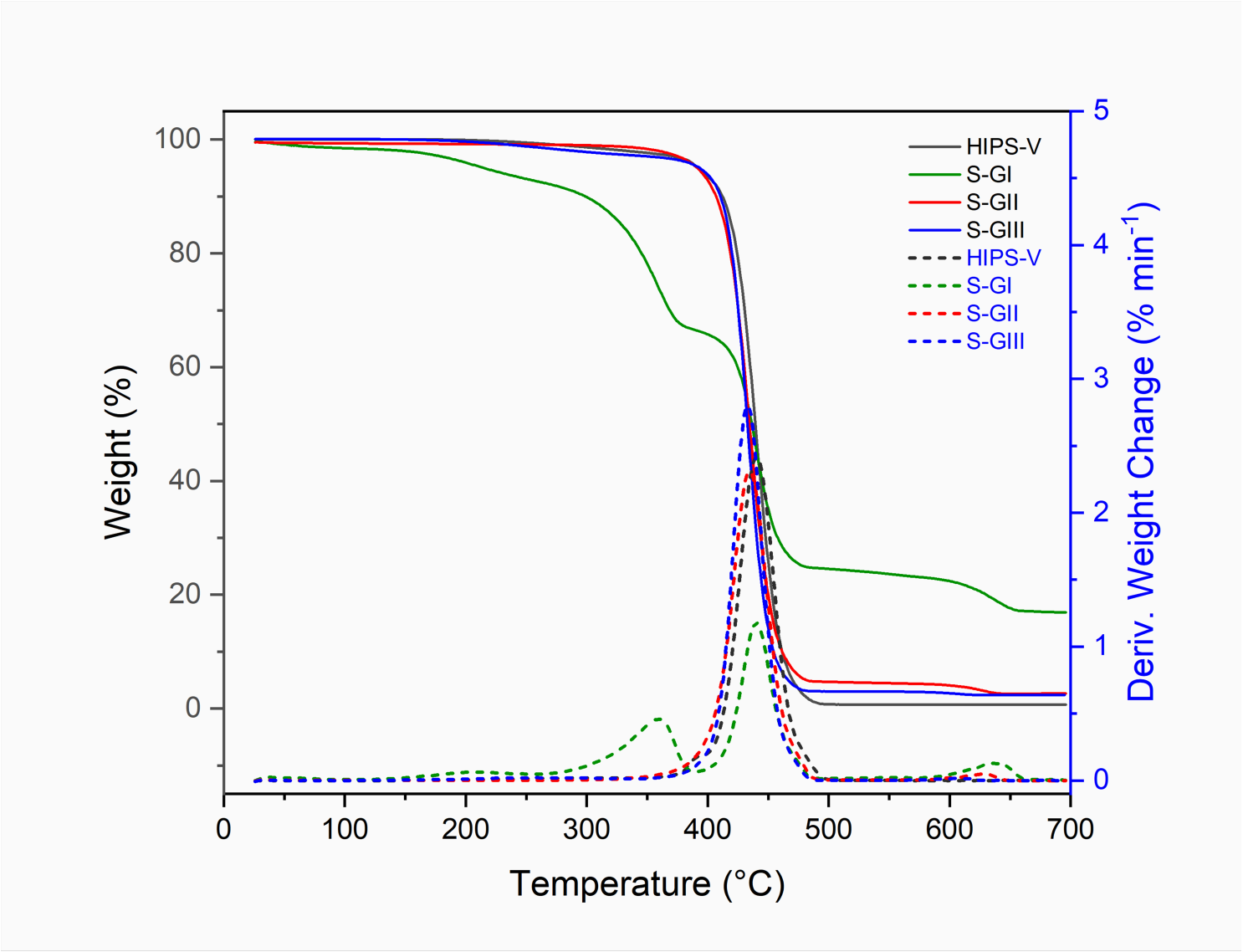


Figure 4

Thermogravimetric curves of clean post-consumer samples (S-GIII), adhesive residue-containing samples (S-GII), and label-containing samples (S-GI) from Soprole cups. HIPS-V is also graphed.

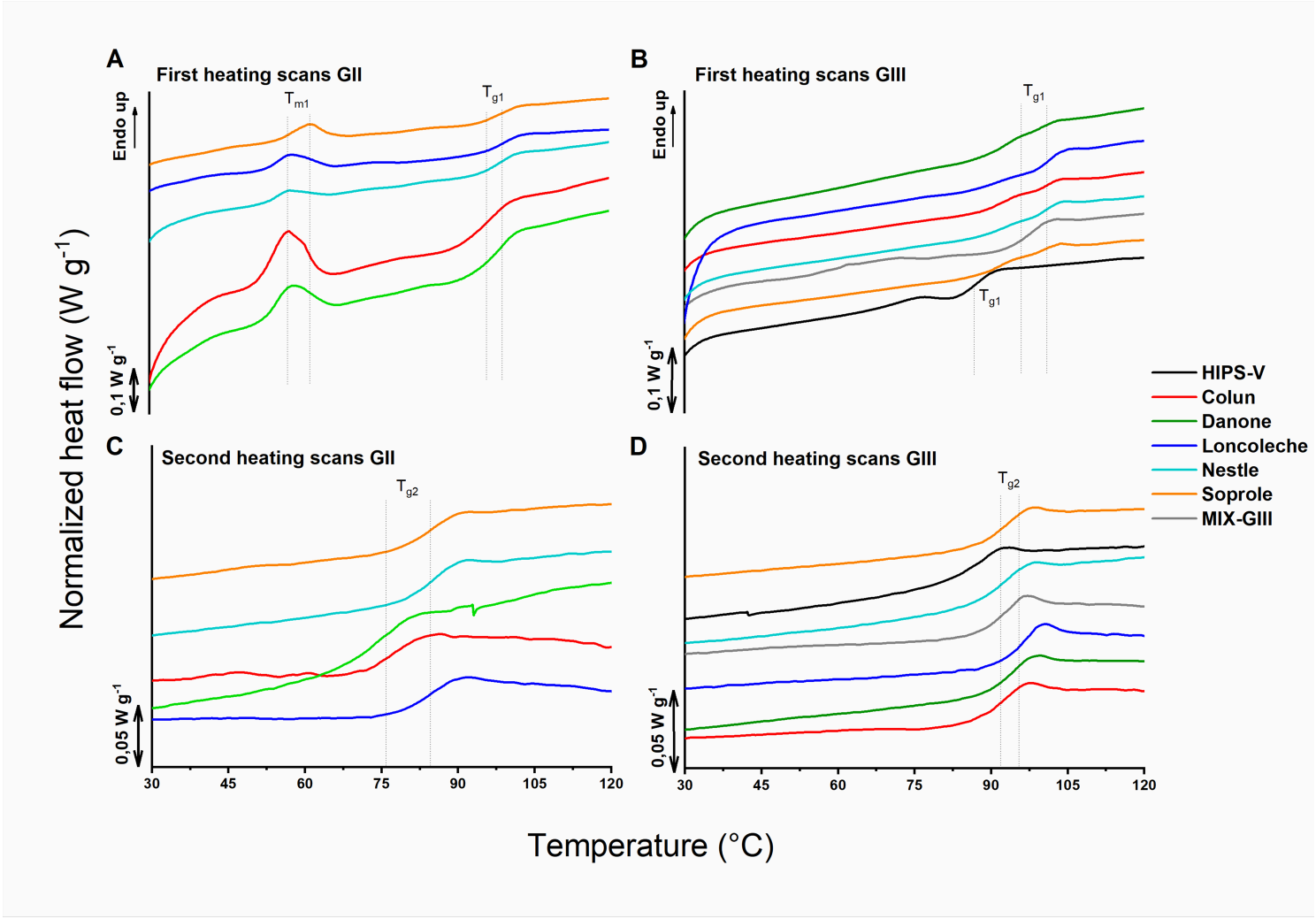


Figure 5

DCS curves of the first (a and b) and second (c and d) heating of virgin and postconsumer HIPS samples. The postconsumer HIPS samples correspond to adhesive residue-containing samples (Group II) and clean samples (Group III).

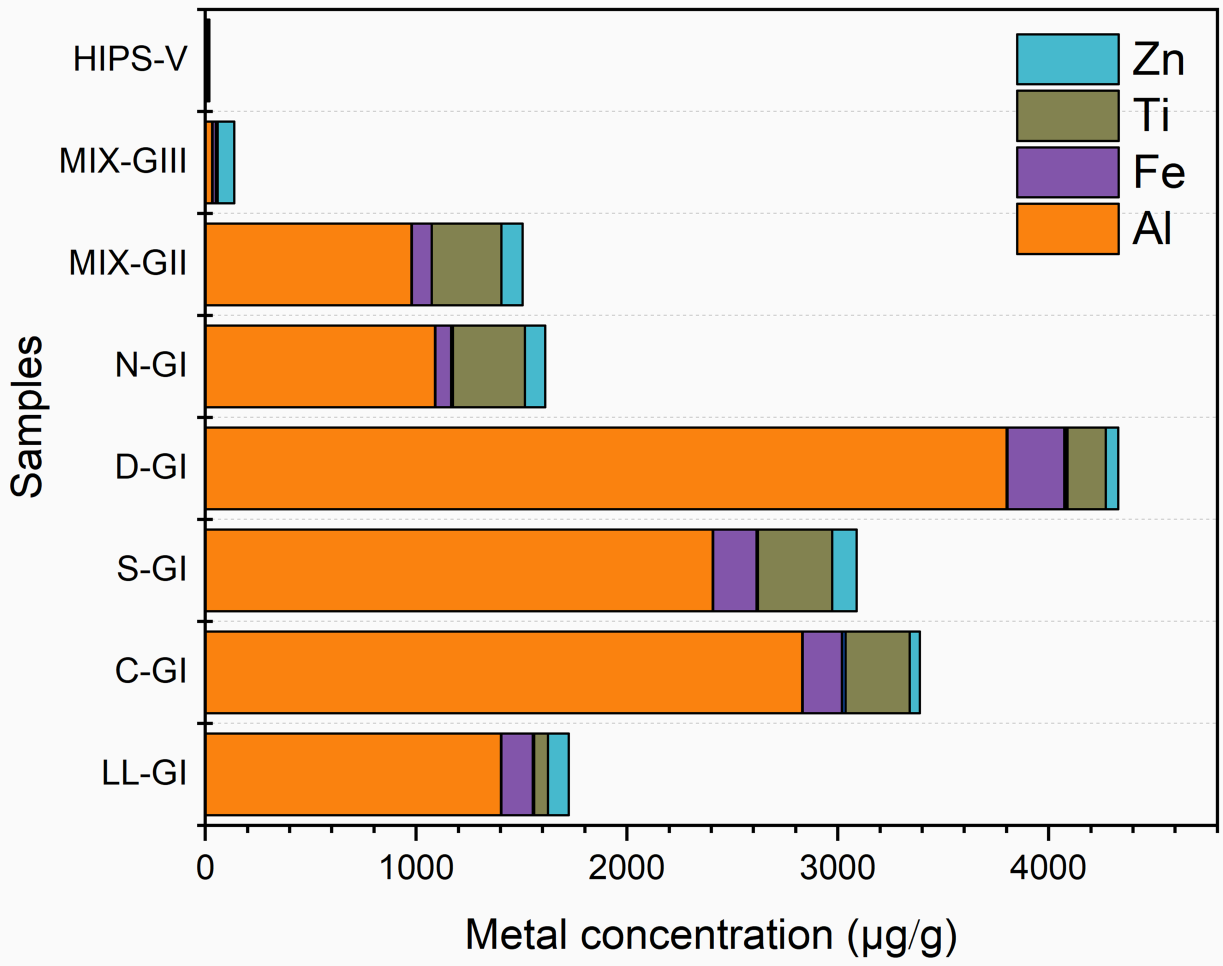


Figure 6

Metal concentration in µg g^{-1} of postconsumer HIPS samples divided into yogurt commercial brands of the label-containing samples (Group I). The mix groups defined in this study for adhesive residue-containing samples (MIX-GII) and post-consumer clean samples (MIX-GIII), as well as virgin HIPS are also included.

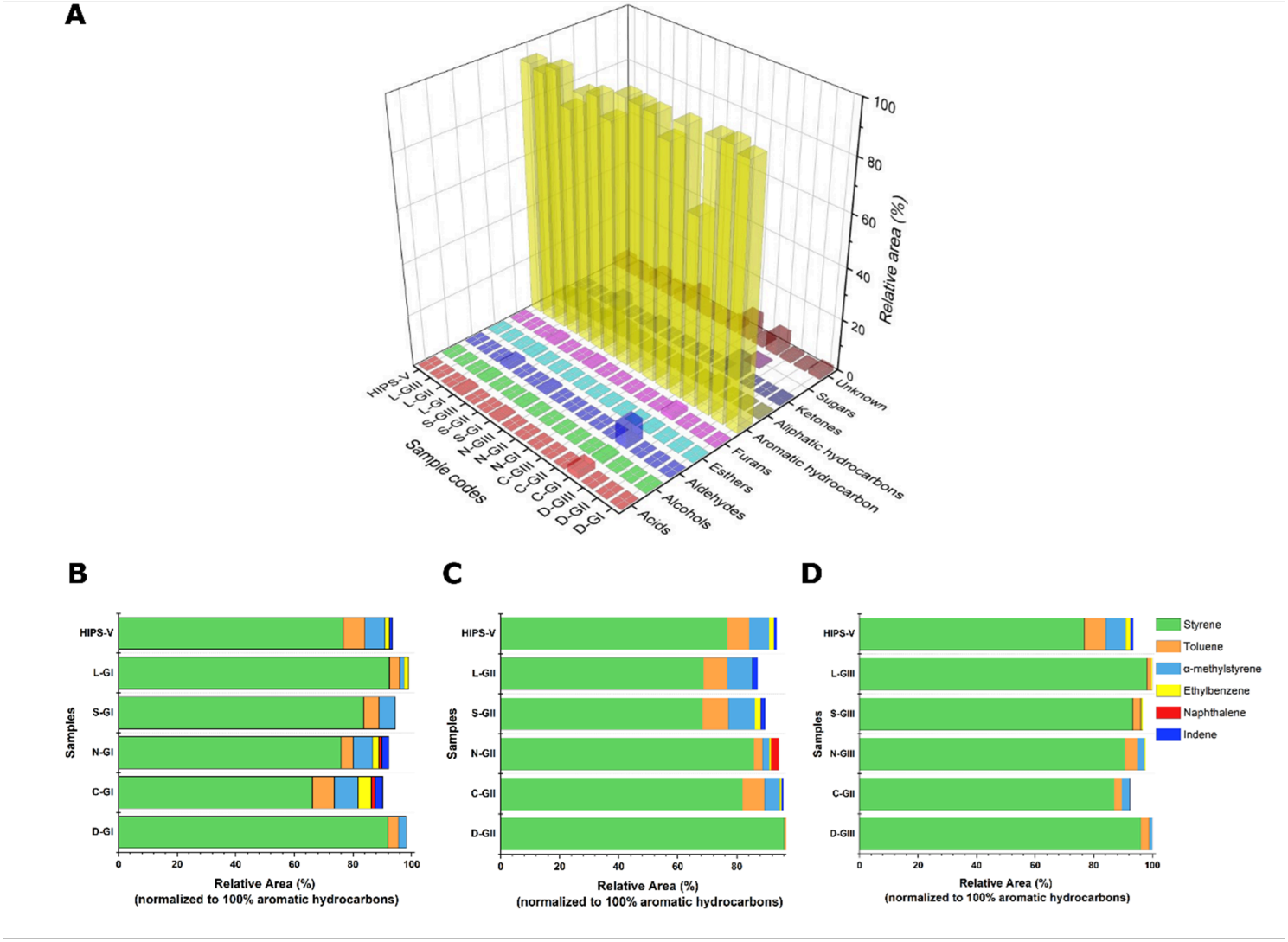


Figure 7

Family product distributions (a) and the five majority compound distributions (b, c and d) of the aromatic hydrocarbon fraction resulting from the thermo-pyrolysis of post-consumer and virgin HIPS.

Supplementary Files

This is a list of supplementary files associated with this preprint. Click to download.

- Supplementarymaterial.docx